JACS
JOURNAL OF THE AMERICAN CHEMICAL SOCIETY
Communication
pubs.acs.org/JACS

Light-Induced Ostwald Ripening of Organic Nanodots to Rods

Sankarapillai Mahesh, Anesh Gopal, Rajasekaran Thirumalai, and Ayyappanpillai Ajayaghosh*

Photosciences and Photonics Group, Chemical Sciences and Technology Division, National Institute for Interdisciplinary Science and Technology, CSIR, Trivandrum-695019, India

Supporting Information

ABSTRACT: Ostwald ripening allows the synthesis of 1D nanorods of metal and semiconductor nanoparticles. However, this phenomenon is unsuccessful with organic π-systems due to their spontaneous self-assembly to elongated fibers or tapes. Here we demonstrate the uses of light as a versatile tool to control the ripening of amorphous organic nanodots (ca. 15 nm) of an azobenzene-derived molecular assembly to micrometer-sized supramolecular rods. A surface-confined dipole variation associated with a low-yield (13−14%) *trans*−*cis* isomerization of the azobenzene moiety and the consequent dipole−dipole interaction in a nonpolar solvent is believed to be the driving force for the ripening of the nanodots to rods.

Formation of one-dimensional (1D) nano- and microstructures is a topic of current interest in the field of advanced materials research.[1] Ostwald ripening is one of the reasons for the formation of 1D nanostructures from nanoparticles of metals and semiconductors.[2] For example, CdTe, CdSe, and ZnO nanoparticles have been shown to form nanorods by an Ostwald-type ripening process.[3] However, controlled ripening of amorphous organic self-assemblies to nano- or microsized supramolecular rods has not been reported. Even though template-assisted synthesis of organic rods is known,[4] template-free preparation of rod-shaped structures of organic molecules with controlled aspect ratio remains challenging. Light is a powerful tool to manipulate the size, shape, and properties of molecules and materials. For example, light has been shown to control the self-assembly of semiconductor nanoparticles into twisted ribbons, which is a rare observation.[5] More widely, light-induced changes of photochromic molecules have been exploited to control properties of molecular, macromolecular, and supramolecular architectures.[6] Among various photochromic molecules, azobenzene has received much attention due to its reversible *trans*−*cis* photoisomerization that proceeds with large dipole moment and volume change, leading to significant modulation of the macroscopic properties.[7]

Herein we report the light-induced reversible morphology change from the initially formed nanodots of a *trans*-azobenzene derivative to supramolecular rods. For the self-assembly of π-systems to nano- and microrods, it is important to prevent the usually occurring spontaneous extended aggregation of molecules. π-Systems derived from phenyleneethynylene units are appropriate for this purpose since they are known to form spherical or circular assemblies due to weak π-interactions.[8] Therefore, we have designed a molecule **4**, combining the features of phenyleneethynylene and azo moieties. Thus, the azobenzene derivative **4**, by virtue of its weak π-stacking ability, was reluctant to form spontaneous 1D assemblies; instead it formed nanodots. Upon UV light irradiation, in contrast to the usually expected deaggregation,[9] length-controlled supramolecular rods were formed. This phenomenon is attributed to a low-yield *trans*−*cis* photoisomerization leading to surface polarity change, resulting in coalescence of the aggregates to rods through a process akin to the Ostwald ripening of metals and semiconductor nanoparticles.

The *trans*-azobenzene derivative **4** was prepared by the Sonogashira coupling protocol in 45% yield (Scheme 1).[10] The

Scheme 1. Synthesis and Photoisomerization of 4

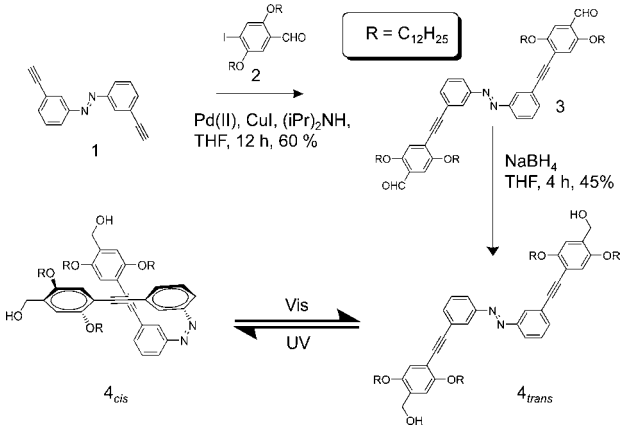

product was characterized by ^{1}H NMR and MALDI-TOF mass spectrometry. The absorption spectrum of **4** in chloroform (1×10^{-5} M) exhibited two distinct maxima, around 280 nm, corresponding to the π−π^* transition of the phenyleneethynylene backbone, and 350 nm, corresponding to the π−π^* transition of the azo moiety (Figure 1a). The absorption spectrum in cyclohexane (1×10^{-5} M) after heating and subsequent cooling to 25 °C showed a low molar extinction coefficient (ε) at 334 nm (27 200 M^{-1} cm^{-1}) when compared to that in chloroform (66 700 M^{-1} cm^{-1}). The intensity of the absorption maximum in cyclohexane is enhanced (ε = 55 900 M^{-1} cm^{-1}) upon heating to 60 °C. The decrease in the ε value in cyclohexane and the subsequent increase with increase in

Received: January 31, 2012
Published: April 14, 2012

   dx.doi.org/10.1021/ja301002g | *J. Am. Chem. Soc.* 2012, 134, 7227−7230

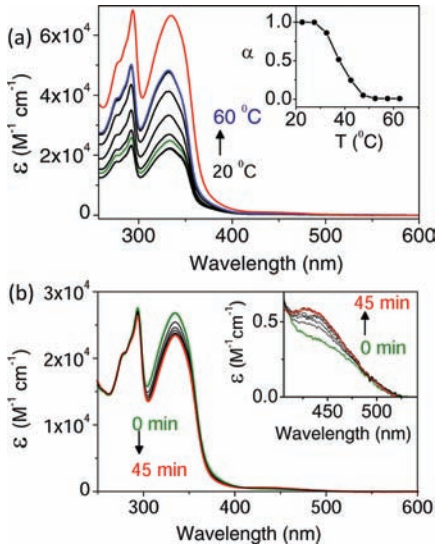

Figure 1. (a) UV/vis absorption spectral changes of **4** (1×10^{-5} M) in chloroform (red), in cyclohexane at 20 °C (black), and in cyclohexane at 60 °C (blue). Inset shows the plot of fraction of aggregates (α) versus temperature (in cyclohexane, λ = 330 nm). (b) Spectral changes of **4** upon photoirradiation in cyclohexane (1×10^{-5} M) using 350 nm light at 25 °C. The inset zooms in on the region between 400 and 525 nm.

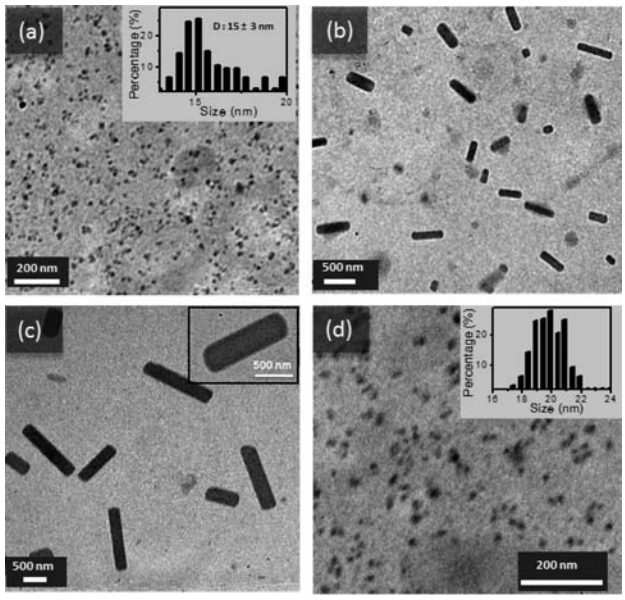

Figure 2. TEM images of the self-assemblies in cyclohexane (1×10^{-4} M). (a) Nanodots of **4** before irradiation. The size distribution is shown in the inset. (b) Transformation of nanoparticles to rods upon irradiation for 10 min and (c) after 1 h with 350 nm light. (d) Reformation of nanodots after heating and cooling of the rods (1 °C/min) followed by irradiation with visible light. TEM images were obtained without staining.

temperature indicate aggregation and deaggregation, respectively, of the molecules. The melting transition temperature (T_m) of the aggregates was 34 °C in cyclohexane.

Irradiation of **4** at 350 nm for 45 min using a band-pass filter ($\lambda_{band\text{-}pass}$ = 350 nm, intensity 0.1 W/cm^2) exhibited a slow decrease in the intensity of the absorption maximum at 335 nm, with the formation of a weak band at 450 nm (Figure 1b). The weak change in the absorption spectrum indicates the low percentage conversion of the *trans* to *cis* isomer. The photoisomerization was further confirmed by the ^{1}H NMR spectral changes in cyclohexane-d_{12} and $CDCl_3$ solvent mixture (1:1 v/v) before and after UV irradiation (Figures S1 and S2). The *trans* isomer showed characteristic peaks at δ = 8.09 (s, ArH, 2H), 7.90 (d, J = 8.4 Hz, ArH, 2H), 7.63 (d, J = 7.9 Hz, ArH, 2H), 7.53 (m, ArH, 2H), 7.01 (s, ArH, 2H), 6.92 (s, ArH, 2H), 4.70 (s, $ArCH_2$, 4H), and 4.03 (m, OCH_3, 8H). Upon UV irradiation, new peaks were formed at δ = 7.36, 7.01, 6.91, and 6.59 due to the formation of the *cis* isomers. The percentage of *trans*–*cis* conversion was calculated from the change in the integration values of the peak at δ = 8.09 with respect to a reference peak δ = 4.03 ppm (m, -OCH_2, 8H), yielding nearly 13% of the *cis* isomers at the photostationary state (PSS).

Transmission electron microscopy (TEM) analysis of the molecule **4** dissolved in cyclohexane (1×10^{-4} M) by heating and subsequent cooling showed the formation of nanodots when the solution was drop-cast on carbon-coated grids (Figure 2a). The size distribution histogram showed an average size of 15 nm (Figure 2a, inset). Surprisingly, after irradiation, the TEM images revealed the complete transformation of the nanodots to supramolecular rods having diameter of 200–400 nm and length of nearly 500 nm to 2 μm (Figure 2b,c). While the width is comparable among different rods, the length showed significant variation with time of irradiation, indicating a pseudo-1D growth process (Figure 2b,c). The high-resolution TEM and the electron diffraction pattern of the rods indicate that they are amorphous in nature (Figure S3). Similarly, powder X-ray diffraction patterns of the nanodots and the rods reveal no long-range periodicity of molecular packing, indicating the absence of any crystalline phase (Figure S4).

For an insight into the photoinduced morphology transition, dynamic light scattering (DLS) analysis was performed in cyclohexane (1×10^{-5} M) before and after irradiation. Initially, aggregates with a hydrodynamic radius (R_h) of around 15 nm were observed (Figure 3a). The corresponding autocorrelation function as a function of the delay time is shown in the inset. After irradiation ($\lambda_{band\text{-}pass}$ = 350 nm, intensity 0.1 W/cm^2 for 45 min), an increase in the R_h value is observed, with an average size of 698 nm (Figure 3a). The autocorrelation function of rods exhibited higher relaxation time when compared to that of the nanodots, reflecting a lower diffusion coefficient for the former. The relatively slower decay of the autocorrelation function with significant deviation indicates considerable changes in the size and morphology of the aggregates. Monitoring of the size variation and size distribution with irradiation shows the time-dependent growth of the particles (Figure 3b). After 10 min irradiation, the particle size has increased significantly with a temporary bimodal distribution, as indicated by the weak signals of the residual particles of the original size, the intensity of which further decreased with continued irradiation.

For further information on the light-induced growth of the dots to rods, zeta potentials were measured before and after photoirradiation in cyclohexane (1×10^{-5} M). It is known that ζ-potential of colloidal particles is a measure of the stability and the size variation, since high ζ-potential value favors better stability and low value indicates rapid coagulation.[11] Surprisingly, the nanodots exhibited an initial average ζ-potential of 30 ± 3 mV (Figure 4a), suggesting that the aggregates have moderate stability in solution. However, upon irradiation with 350 nm light, the average ζ-potential value decreased to −5 ± 3

dx.doi.org/10.1021/ja301002g | J. Am. Chem. Soc. 2012, 134, 7227–7230

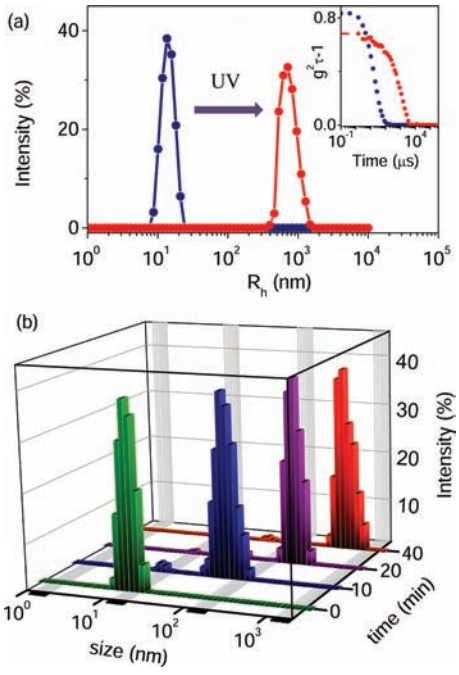

Figure 3. (a) DLS profiles showing the intensity-averaged hydrodynamic radius (R_h) of the self-assemblies before (blue) and after (red) photoirradiation with 350 nm light. The corresponding autocorrelation functions are shown in the inset. (b) DLS histogram showing the particles' size growth upon intervals of photoirradiation.

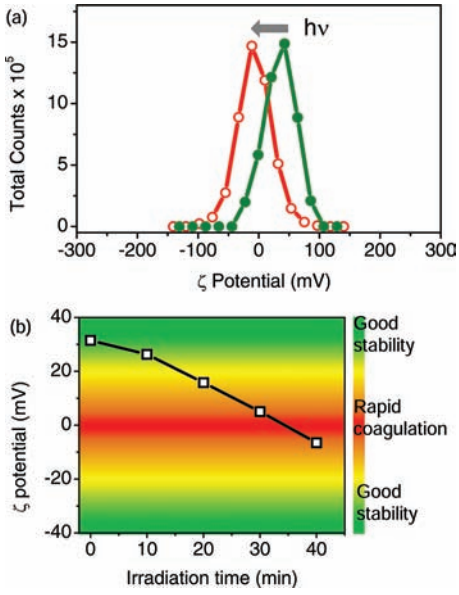

Figure 4. (a) Zeta potential variation of **4** before (green) and after (red) irradiation. (b) Time-dependent ζ-potential variation of the molecules with respect to irradiation time.

mV. The decrease in the ζ-potential value upon the light-induced isomerization, as evident in Figure 4b, may facilitate agglomeration of the individual aggregate, leading to the growth of rods, as supported by the TEM images.

The rods could be converted back to dots by heating the former to 60 °C followed by cooling at a rate of 1 °C/min under irradiation with visible light. DLS analysis of the reversible process showed a decrease of the hydrodynamic radii (Figure S5) due to nanodots formation which is further confirmed by TEM analysis (Figure 2d). Similarly, the ζ-potential values exhibited significant variation upon heating and cooling followed by visible light irradiation. These changes are reversible for several cycles of UV and visible light irradiations (Figure S6).

The above observations were surprising since, in the case of azo-linked molecules, *trans*−*cis* isomerization is known to disrupt or weaken the self-assembly, as reported in several cases.[9] In the present case, the low photoisomerization yield (13%) has become advantageous for the observed morphology transition. The situation would have been different in the case of an efficient isomerization of the *trans* to the *cis* form. Our attempt to isolate the *cis* isomer to study its aggregation behavior was not successful due to the fast thermal back-isomerization to the *trans* form. The reason for the low yield of the *cis* isomer could be related to structural as well as morphological features of **4**. The phenyleneethynylene moieties may partly interfere with the light absorption by the azo moieties in **4**, which may decrease the efficiency of isomerization. In addition, light filtration by the phenyleneethynylene moieties may decrease the light absorption by molecules present in the inner part of the nanodots, preventing their isomerization.

We hypothesize that the mechanism of the rod formation may involve a surface interaction pathway associated with a time-dependent, light-driven process as shown in Figure 5.

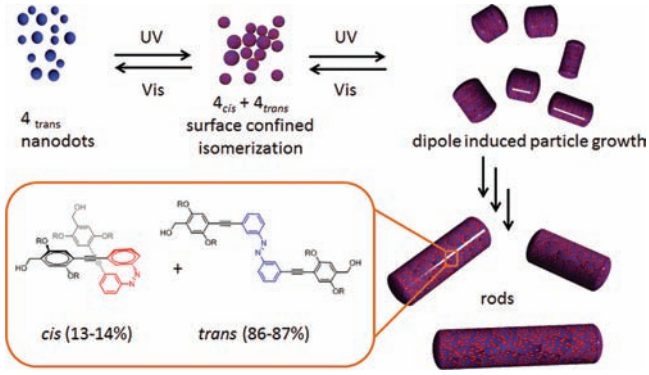

Figure 5. Schematic representation of the light-driven ripening of nanodots to rods. The surface-confined *trans*−*cis* isomerization is indicated by the red color on the dots and rods. At the PSS, rods have 13−14% *cis* content.

Upon UV irradiation of the nanodots, the $\mathbf{4}_{trans}$ is converted to the $\mathbf{4}_{cis}$ in low yields (13−14%), which is restricted to the surface of the dots. Therefore, the local concentration of $\mathbf{4}_{cis}$ on the surface of the dots will be high, which in turn enhances the surface dipole moment since each *trans*−*cis* isomerization of the azobenzene may contribute a dipole moment change of $\mu \approx 0.52$ D for the *trans* to $\mu \approx 5$ D for the *cis*. Such a large increase in the dipole moment after irradiation changes the ζ-potential of the nanodots (30 ± 3 mV) toward an instability regime (−5 ± 3 mV), which facilitates interparticle association, leading to a rod-shaped structural transformation. The *cis* content in the rods obtained after 40 min irradiation was ca. 13−14%, as estimated from the change in the UV−vis spectra. The observed morphology evolution of the dots to rods can therefore be corroborated to the surface-confined dipole moment change associated with the *trans*−*cis* isomerization and the consequent ζ-potential variation of the initially formed molecular aggregates.

dx.doi.org/10.1021/ja301002g | *J. Am. Chem. Soc.* 2012, 134, 7227−7230

The above suggested mechanism is well supported by recent reports on the effect of the surface polarity difference of azobenzene monolayers on gold nanoparticles, as reported by Grzybowski and co-workers.[12] In another report, Ikegami et al. showed that passivated ultrathin Nb films containing azo chromophores exhibit significant changes in their superconductivity upon photoirradiation.[13] In both cases, the observed property changes are attributed to the change in the surface dipole moment as a result of the photoinduced *trans*−*cis* isomerization. Thus, the weak electrostatic repulsion of the aggregates is overcome by the relatively strong dipole−dipole interaction. The preferential 1D growth may be controlled by the mass transport through the surface equilibrium of the *cis* and the *trans* isomers. The large surface area on the top and bottom faces of the nanodots allows longitudinal growth, leading to pseudo-1D rods, similar to the Ostwald ripening of metal and semiconductor nanoparticles. It is believed that the initially formed nanodots morphology and the polarity of the solvents play crucial roles in the formation of rods. To prove this argument, we conducted experiments in chloroform and tetrahydrofuran. In both solvents, even though aggregates are formed before and after irradiation, they were not exactly the nanodots or rods as observed in cyclohexane (Figures S7). However, in chloroform-cyclohexane mixture (1:1, v/v) nanodots and rods were formed before and after irradiation, indicating that the addition of a nonpolar solvent facilitates the photoinduced ripening process (Figure S8).

This method allows the preparation of organic supramolecular rods without using templates, which can be assembled and disassembled by light of appropriate wavelengths. The new observation described here reveals yet another property of the versatile azobenzene chromophore, which may inspire further studies en route to stimuli-responsive hierarchical structures with controlled morphological features.

■ ASSOCIATED CONTENT

Supporting Information

Synthetic procedures, characterizations, experimental details, and NMR, DLS, TEM, and XRD data. This material is available free of charge via the Internet at http://pubs.acs.org.

■ AUTHOR INFORMATION

Corresponding Author

ajayaghosh62@gmail.com

Notes

The authors declare no competing financial interest.

■ ACKNOWLEDGMENTS

A.A. is grateful to the Department of Atomic Energy, Government of India, for a DAE-SRC Outstanding Researcher Award. S.M is thankful to Universities Grants Commission for a Fellowship. A.G. and R.T. are thankful to CSIR for fellowships.

■ REFERENCES

(1) (a) Whitesides, G. M.; Grzybowski, B. *Science* **2002**, *295*, 2418. (b) Grzybowski, B. A.; Winkleman, A.; Wiles, J. A.; Brumer, Y.; Whitesides, G. M. *Nat. Mater.* **2003**, *2*, 241. (c) Tang, Z. Y.; Kotov, N. A. *Adv. Mater.* **2005**, *17*, 951. (d) Ariga, K.; Hill, J. P.; Lee, M. V.; Vinu, A.; Charvet, R.; Acharya, S. *Sci. Tech. Adv. Mater.* **2008**, *9*, 14109. (e) Srivastava, S.; Kotov, N. A. *Soft Matter* **2009**, *5*, 1146.

(2) (a) Ostwald, W. *Lehrbuch der Allgemeinen Chemie*; Leipzig, Germany, 1896; Vol. 2, part 1. (b) Redmond, P. L.; Hallock, A. J.; Brus, L. E. *Nano Lett.* **2004**, *5*, 131. (c) Liu, B.; Zeng, H. C. *Small* **2005**, *1*, 566. (d) Noorduin, W. L.; Vlieg, E.; Kellogg, R. M.; Kaptein, B. *Angew. Chem., Int. Ed.* **2009**, *48*, 9600.

(3) (a) Spanhel, L.; Anderson, M. A. *J. Am. Chem. Soc.* **1991**, *113*, 2826. (b) Tang, Z.; Kotov, N. A.; Giersig, M. *Science* **2002**, *297*, 237. (c) Pacholski, C.; Kornowski, A.; Weller, H. *Angew. Chem., Int. Ed.* **2002**, *41*, 1188. (d) Tang, Z. Y.; Wang, Y.; Shanbhag, S.; Giersig, M.; Kotov, N. A. *J. Am. Chem. Soc.* **2006**, *128*, 6730. (e) Li, R.; Luo, Z.; Papadimitrakopoulos, F. *J. Am. Chem. Soc.* **2006**, *128*, 6280.

(4) (a) Deirdr, O.; Ingo, L.; Gareth, R. *Nature Nanotechnol.* **2007**, *2*, 180. (b) Rabih, O. A-K.; Christopher, J. B. *Chem. Commun.* **2006**, 1224.

(5) Srivastava, S.; Santos, A.; Critchley, K.; Kim, K.-S.; Podsiadlo, P.; Sun, K.; Lee, J.; Xu, C.; Lilly, G. D.; Glotzer, S. C.; Kotov, N. A. *Science* **2010**, *327*, 1355.

(6) (a) Ichimura, K.; Oh, S. K.; Nakagawa, M. *Science* **2000**, *288*, 1624. (b) Jousselme, B.; Blanchard, P.; Gallego-Planas, N.; Delaunay, J.; Allain, M.; Richomme, P.; Levillain, E.; Roncali, J. *J. Am. Chem. Soc.* **2003**, *125*, 2888. (c) Yu, Y. L.; Nakano, M.; Ikeda, T. *Nature* **2003**, *425*, 145. (d) Lendlein, A.; Jiang, H. Y.; Junger, O.; Langer, R. *Nature* **2005**, *434*, 879. (e) Ikeda, T.; Mamiya, J.-i.; Yu, Y. *Angew. Chem., Int. Ed.* **2007**, *46*, 506. (f) Yagai, S.; Kitamura, A. *Chem. Soc. Rev.* **2008**, *37*, 1520. (g) Juan, M. L.; Plain, J.; Bachelot, R.; Royer, P.; Gray, S. K.; Wiederrecht, G. P. *ACS Nano* **2009**, *3*, 1573. (h) Zeitouny, J.; Aurisicchio, C.; Bonifazi, D.; De Zorzi, R.; Geremia, S.; Bonini, M.; Palma, C. A.; Samori, P.; Listorti, A.; Belbakra, A.; Armaroli, N. *J. Mater. Chem.* **2009**, *19*, 4715. (i) Hosono, N.; Kajitani, T.; Fukushima, T.; Ito, K.; Sasaki, S.; Takata, M.; Aida, T. *Science* **2010**, *330*, 808. (j) Tamesue, S.; Takashima, Y.; Yamaguchi, H.; Shinkai, S.; Harada, A. *Angew. Chem., Int. Ed.* **2010**, *49*, 7461. (k) Xie, T. *Nature* **2010**, *464*, 267. (l) Nguyen, T. T.; Turp, D.; Wang, D.; Nolscher, B.; Laquai, F.; Mullen, K. *J. Am. Chem. Soc.* **2011**, *133*, 11194.

(7) (a) Kumar, G. S.; Neckers, D. C. *Chem. Rev.* **1989**, *89*, 1915. (b) Ichimura, K. *Chem. Rev.* **2000**, *100*, 1847. (c) Crecca, C. R.; Roitberg, A. E. *J. Phys. Chem. A* **2006**, *110*, 8188.

(8) (a) Ajayaghosh, A.; Varghese, R.; George, S. J.; Vijayakumar, C. *Angew. Chem., Int. Ed.* **2006**, *45*, 1141. (b) Ajayaghosh, A.; Varghese, R.; Mahesh, S.; Praveen, V. K. *Angew. Chem., Int. Ed.* **2006**, *45*, 7729. (c) Yagai, S.; Mahesh, S.; Kikkawa, Y.; Unoike, K.; Karatsu, T.; Kitamura, A.; Ajayaghosh, A. *Angew. Chem., Int. Ed.* **2008**, *47*, 4691. (d) Fernandez, G.; Garcia, F.; Sanchez, L. *Chem. Commun.* **2008**, 6567. (e) Yoosaf, K.; Belbakra, A.; Armaroli, N.; Llanes-Pallas, A.; Bonifazi, D. *Chem. Comm* **2009**, 2830. (f) García, F.; Aparicio, F.; Fernández, G.; Sánchez, L. *Org. Lett.* **2009**, *11*, 2748. (g) García, F.; Fernández, G.; Sánchez, L. *Chem.—Eur. J.* **2009**, *15*, 6740.

(9) (a) Murata, K.; Aoki, M.; Suzuki, T.; Harada, T.; Kawabata, H.; Komori, T.; Ohseto, F.; Ueda, K.; Shinkai, S. *J. Am. Chem. Soc.* **1994**, *116*, 6664. (b) Yagai, S.; Nakajima, T.; Karatsu, T.; Saitow, K.-i.; Kitamura, A. *J. Am. Chem. Soc.* **2004**, *126*, 11500. (c) Tong, X.; Wang, G.; Soldera, A.; Zhao, Y. *J. Phys. Chem. B* **2005**, *109*, 20281.

(10) Sonogashira, K.; Tohda, Y.; Hagihara, N. *Tetrahedron Lett.* **1975**, *16*, 4467.

(11) (a) Booth, F. *Nature* **1948**, *161*, 83. (b) Xu, R. L.; Wu, C. F.; Xu, H. Y. *Carbon* **2007**, *45*, 2806. (c) Capito, R. M.; Azevedo, H. S.; Velichko, Y. S.; Mata, A.; Stupp, S. I. *Science* **2008**, *319*, 1812.

(12) (a) Klajn, R.; Bishop, K. J.; Fialkowski, M.; Paszewski, M.; Campbell, C. J.; Gray, T. P.; Grzybowski, B. A. *Science* **2007**, *316*, 261. (b) Klajn, R.; Bishop, K. J.; Grzybowski, B. A. *Proc. Natl. Acad. Sci. U.S.A.* **2007**, *104*, 10305. (c) Klajn, R.; Wesson, P. J.; Bishop, K. J. M.; Grzybowski, B. A. *Angew. Chem., Int. Ed.* **2009**, *48*, 7035.

(13) Ikegami, A.; Suda, M.; Watanabe, T.; Einaga, Y. *Angew. Chem., Int. Ed.* **2010**, *49*, 372.